Computational fluid dynamics simulation of the turbulence models in the tested section on wind tunnel

by Budhi Suyitno

Mechanical Engineering

Computational fluid dynamics simulation of the turbulence models in the tested section on wind tunnel

Ismail [a],[*], Johanis John [b], Erlanda A. Pane [a], Budhi M. Suyitno [a], Gama H.N.N. Rahayu [c], Damora Rhakasywi [d], Agri Suwandi [a]

[a] Department of Mechanical Engineering, Faculty of Engineering, Universitas Pancasila, Jl. Srengseng Sawah, Jagakarsa, Jakarta Selatan 12640, Indonesia
[b] Mechanical Engineering Postgraduate Student, Faculty of Engineering, Universitas Pancasila, Jl. Srengseng Sawah, Jagakarsa, Jakarta Selatan 12640, Indonesia
[c] Department of Industrial Engineering, Faculty of Engineering, Universitas Pancasila, Jl. Srengseng Sawah, Jagakarsa, Jakarta Selatan 12640, Indonesia
[d] Department of Mechanical Engineering, Faculty of Engineering, UPN Veteran Jakarta, Jl. Rs. Fatmawati, Pondok Labu, Jakarta Selatan, DKI Jakarta, 12450, Indonesia

ABSTRACT

The application of the computational fluid dynamic method with several turbulence models to obtain the right and ideal position of the test object in the test room has been carried out by analyzing the pattern of velocity distribution, pressure distribution and intensity of fluid turbulence in an open type subsonic wind tunnel test chamber. The reason is that the wind tunnel is made not following the usual design procedures, but it is more prioritizes the design of the test chamber and other parts. The turbulence model used is the k-ϵ model, k-ω model, RSM model, SST k-ω model, and LES model. The simulation results give the lowest test room turbulence intensity given by the k-ϵ model which is 0.8% while the highest is given by the LES model of 11%.

1. Introduction

Wind tunnels are useful in understanding the theory of aerodynamics, fluid flow characters, and turbulence, which ultimately leads to product optimization. Along with the increasing need for test data, the differentiation of the field of technology engineering, and the increasing size of test samples, wind tunnels continue to be developed and modified both open-loop and closed-loop types to become new and ideal wind tunnels so that they can meet the needs of laboratory testing [1].

Optimization of subsonic wind tunnel design was carried out in previous studies [2–4], but it needs to be reviewed before it is made. Particularly the distribution of fluid flow in the test chamber is important to get an idea of how much laminar flow can occur, which part of the test room is possible fluctuations in airflow which will affect the airflow around the test object later. The CFD (computational fluid dynamic) method has become the main choice to be used to explore the shape and character of fluid flow, as in a wind tunnel. Thus the picture obtained will be closer to the real condition, errors that arise from modeling also become smaller and can be tolerated.

The intensity of turbulence, the distribution pattern of fluid flow, velocity and pressure distribution, etc. can be obtained from the turbulence models contained in the CFD method. The turbulence models include the k-ϵ model with several adjustments, the k-ω model, the Spalart-Allmaras model, the LES model, the RSM model, and several other models that are still being developed to get the shape closer to the real conditions. So in this study, the turbulence models are combined to obtain a detailed position or area in the wind tunnel that produces laminar flow potential, especially in the test chamber. How big is the intensity of turbulence that is possible and the width of the area that has a uniform wind speed and is laminar. As much as possible the area does not experience fluctuations in air flow.

The k-ε model purposed is to predict airflow away from wall or surface [5,6] because this model calculates factor turbulence kinetic energy k and dissipation energy ε. The k-ε turbulence model has been used in simulating the distribution and relations of air flowing in the presence of buildings [7,8] but by modeling based on RNG and Launder-Kato modeling [9]. Another result is

the emergence of separate airflow and secondary airflow (secondary flow motion). Due to predict airflow nearest the wall or surface, the k-ω model is implemented. This model calculate freestream value w_f, makes it sensitive to the flow near the wall or surface [10].

To anticipate changes in pressure that might occur in wind trough, the RSM model is used. The RSM model calculates the pressure-strain of each unit in all directions and compared as the rate of velocity change, convection, production, dissipation, redistribution of vortex flow [11,12] also the presence of separation-flow due to boundary layer collision [13]. Even though, the RSMs model is based on transport equations $\overline{u_i u_j}$ and ε so it has a lack in some ways but the RMS model is feasible for asymmetric turbulence phenomena [14]. The SST k-ω model approach is used because of its sensitivity to the area near the wall due to the pressure-stress of airflow fluctuation, as well as the changing effect of velocity and temperature [15].

In addition to studying the pattern of pressure distribution, velocity and temperature due to transient flow, there is still a study of turbulence models, namely the LES model. LES has advantages in modeling turbulence at high Reynolds numbers and being a comparative material for other models [16]. Furthermore, simulating examples of flow collisions that occur in the combustion chamber, in the models contained in the Scale Subgrid method such as the Smagorinsky model form, Dynamic Smagorinsky, WALE model and turbulent kinetic energy subgrid model [17].

In the first example of this study, it was explained that the design flow was changed, not following the existing design methods, except by designing the test chamber first [2]. The size and shape of the test chamber are made maximum so that it can provide test models to a definite size. While other spaces are accord with the remaining size of available space, consequently the ratio of contraction space and diffusion space may not be standard. In other words, the contraction and diffusion area may not have ideal turbulence levels.

In general, in addition to testing existing wind tunnel designs, this study also examined the distribution of fluid velocity, pressure, and intensity of turbulence in wind tunnels using five different turbulence models to determine the exact position of the optimal test sample, an area in the space test that is not affected by fluctuations in velocity and fluid pressure. To improve the results of the study in this CFD method, various turbulence models, such as k-ε model, k-ω model, RSMs model, SST k-ω and the LES model was utilized. The first four models (model k-ε, model k-ω, SST k-ω, LES model) use the eddy viscosity equation while the second model is the RSM model using the Reynolds stress transport equation. Thus the superiority of each model will complement each other in getting a picture of the pattern of fluid flow distribution in the test chamber. The compilation results of turbulence models are used to determine the exact and the optimal position of the sample inside the test chamber or could be a reason for changing the geometric structure of the wind tunnel.

2. Turbulence models

The airflow is modeled with several turbulence models to ensure the precision of the wind tunnel that will be made later. The model includes the standard k-ε, k-ω standard, SST k-ω model, RSM model, and LES model. The intensity of turbulence is obtained from strong turbulence and is a statistical process in the form of $\tilde{u}_i = \sqrt{\overline{u'_i(t)^2}}$, then Equation (1) is obtained as the intensity of turbulence TI without dimensions [18].

$$TI = \left(\tilde{u}_i / \bar{u}_i \right) \tag{1}$$

while $\bar{u}_i$ is average velocity, u'_i is velocity fluctuation, and for $TI \leq 1\%$ as low turbulence and $TI \geq 10\%$ as fully turbulence.

Airflow turbulence analysis in this design study was carried out based on the form of Equations 2 and 3 or also called the Navier Stokes transport equation [19].

$$\text{Conservation of mass}: \frac{\partial \rho}{\partial t} + \frac{\partial}{\partial x_j}\left(\rho u_j \right) = 0$$

$$\text{Conservation of momentum}: \frac{\partial \rho u_t}{\partial t} + \frac{\partial \rho u_i u_j}{\partial x_j}$$
$$= -\frac{\partial p}{\partial x_i} + \frac{\partial \sigma_{ij}}{\partial x_j} standark + F_i$$

2.1. Standard k-ε model

The standard k-ε model will determine the amount of turbulent kinetic energy k (energy transport) and the kinetic dissipation rate ϵ as a represent of turbulence diffusion according to the Boussinesq hypothesis written in Eq. (4) [20].

$$\frac{\partial}{\partial t}(\rho k) + \frac{\partial}{\partial x_i}(\rho k u_i) = \frac{\partial}{\partial x_j}\left[\left(\mu + \frac{\mu_t}{\sigma_k} \right) \frac{\partial k}{\partial x_j} \right] + P_k + P_b - \rho\epsilon - Y_M + S_k \tag{4}$$

Assuming the Reynolds number is very large or applies absolute turbulent assumptions (full turbulent), then factor Y_M by $Y_M = 2\rho\epsilon\frac{k}{a_t^2}$ in Equation (4) can be ignored for incompressible fluids. This model has robustness for describing airflow far from the wall.

2.2. Standard k-ω model

This model consists of the factor k as turbulent kinetic energy and factor ω as the exact rate of dissipation (specific dissipation rate) [21,22], where $\omega \approx \epsilon/k$. Turbulent kinetic energy and the rate of dissipation are certainly written in the form of Eq. (5) [20].

$$\frac{\partial}{\partial t}(\rho\omega) + \frac{\partial}{\partial x_j}(\rho u_j\omega) = \alpha\frac{\omega}{k}\rho\tau_{ij}\frac{\partial u_i}{\partial x_j} - \beta\rho\omega^2 + \sigma_d\frac{\rho}{\omega}\frac{\partial k}{\partial x_j}\frac{\partial\omega}{\partial x_j} + \frac{\partial}{\partial x_j}\left[\left(u + \sigma\frac{\rho k}{\omega} \right)\frac{\partial\omega}{\partial x_j} \right] \tag{5}$$

This model offered accuracy of prediction for free shear flows.

2.3. SST k-ω model

The SST k-ω model (Eq. (6) [20]) tends to model turbulence near the wall as a consequence of the friction between the fluid and the field it passes at the high price of the Reynolds number.

$$\frac{\partial}{\partial t}(\rho\omega) + \frac{\partial}{\partial x_j}(\rho\omega u_i) = \frac{\partial}{\partial x_j}\left(\Gamma_\omega\frac{\partial\omega}{\partial x_j} \right) + G_\omega - Y_\omega + D_\omega + S_\omega \tag{6}$$

With, turbulent kinetic energy produced is $G_k = min(G_k, 10\rho\beta^*k\omega)$ and kinetic energy dissipation k is $Y_k = \rho\beta^*k\omega$. S is the amount of flow strain rate in the tunnel.

2.4. RSM model

The basic concept of the RSM model (Equation (7) [23]) is the same as the eddy viscosity model (k-ε model, k-ω model, SST k-ω model), but the pressure-strain is immediately partially resolved.

$$\frac{\partial}{\partial x_k}\left(\rho u_k \overline{u_i' u_j'}\right) = \frac{\partial}{\partial x_k}\left(\frac{\mu_t}{\sigma_k}\frac{\partial \overline{u_i' u_j'}}{\partial x_k}\right) + \frac{\partial}{\partial x_k}\left[\mu \frac{\partial}{\partial x_k}\left(\overline{u_i' u_j'}\right)\right]$$
$$- \rho\left(\overline{u_i' u_k'}\frac{\partial u_j}{\partial x_{kP_{ij}}} + \overline{u_j' u_k'}\frac{\partial u_i}{\partial x_k}\right) + \Phi_{ij} - \frac{2}{3}\delta_{ij}\rho\epsilon \qquad (7)$$

2.5. LES model

The LES model uses a filter that is passing a small turbulence energy to the average and modeling it. This method is called subgrid-scale modeling, calculated based on Equation 8 [20] with SGS viscosity $\frac{\partial \overline{y}_i}{\partial x_j} = 0$.

by,

$$\frac{\partial \overline{u}_i}{\partial t} + \frac{\partial \overline{u}_i \overline{u}_j}{\partial x_j} = \delta_{li} - \frac{1}{\rho}\frac{\partial \overline{p}}{\partial \overline{x}_i} + \frac{\partial}{\partial \overline{x}_j}\left[\frac{\partial \overline{u}_i}{\partial x_j}(v + v_T)\right]$$

3. CFD method

The computational method uses commercial Ansys Fluent Release 15. The airflow is assumed friction absence because the test chamber material is from acrylic. In spite of this, the flow is chosen to move in three dimensions, incompressible with the flow in the tunnel considered fully-turbulent. Although the geometry of the wind tunnel is symmetrical so that the meshing is sufficiently structured, but to get the fluctuation of air flow in the wind tunnel can be guaranteed then the unstructured meshing is chosen (Fig. 2). The use of unstructured meshing sacrifices CPU speed in processing data, but the accuracy of the simulation can be guaranteed. The transient flow form was chosen in the simulation because of the wind tunnel section (contraction chamber and diffusion chamber) that did not have a standard ratio. With transient mode, the possibility of 3D air movement in the wind tunnel can be anticipated.

Some turbulence models used are the standart k-ϵ model, k-ω model, SST k-ω model, RSMs model, and LES model. The k-ϵ model leads to examine near the with a standard wall function ($30 < y^+ \langle 300$), whereas the k-ω model is assigned to set about the standard wall function ($y^+ \langle 10$). However, a low Reynolds number correction pertain to SST k-ω model, then the SST k-ω model is a combination of the advantages of the k-ω model in delineating the phenomena that come about near the wall with the stability of the k-ϵ model in defining a flow in conditions far from the wall. The RSM model has known as a model of high Reynolds number because the pressure strain effect and this model were used to illustrate separation flow, flows with recirculation zone which could ascend in simulation [24]. Particularly in the average movement of air flow velocity will be divided into three, which is the occurrence of compression, acceleration and then experiencing expansion.

The pressure and momentum equation is carried off using the SIMPLE algorithm (Semi Implicit Method for Pressure-Linked Equations). This scheme as an alternative to compensate for the computational disadvantage by using specific turbulence models.

The contracting room control variable against the passageway is the dimension of input geometry in the form of area, length of con-
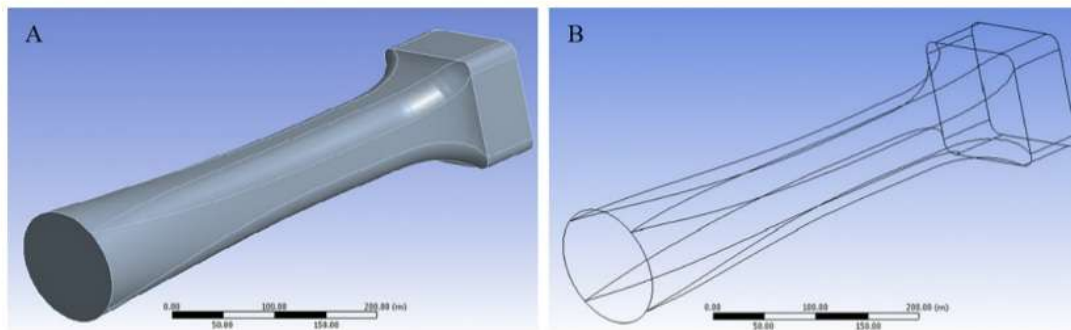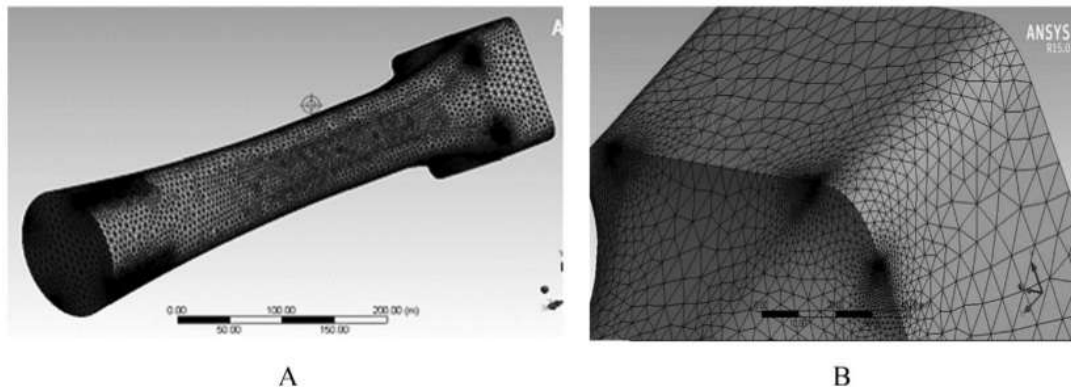

Fig. 1. Wind tunnel by ANSYS® 15.0.

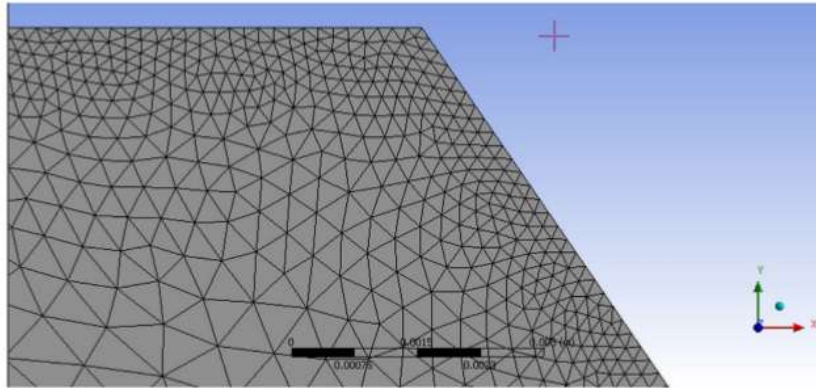**Fig. 2.** (A) meshing. (B) Angle magnification.

Fig. 3. Corner 2D Meshing.

traction space, area of output hole and contraction ratio. The wind tunnel meshing in Fig. 2 is arranged close to 10^{-4} m with a tolerance of 0.06 m resulting in $\sim 10^5$ grids and 198,387 nodes and its used for all models. Thus capturing turbulent conditions near the wall represented by y^+ requires special attention. Mesh density and mesh structure affect this requirement and some of it has been explained in the previous.

The relationship of the initial number of cells to the size of wind tunnel can be determined by the relationship given by $N = 44,400 \times V^{0.38}$ where N is the number of cells and V is the volume in m^3 [25]. Assuming a minimum wall function y^+ is 30, the wall spacing is around 0.28 mm and applies to the $k\text{-}\epsilon$ model and the RSMs model. While the other models are assumed to have the same wall function as the two models above, because these values are still in the log wall region (Fig. 3).

4. Boundary conditions

The reference pressure used is the normal room pressure or static pressure $p_0 = 101325$ Pa (760 mmHg) with the airflow velocity
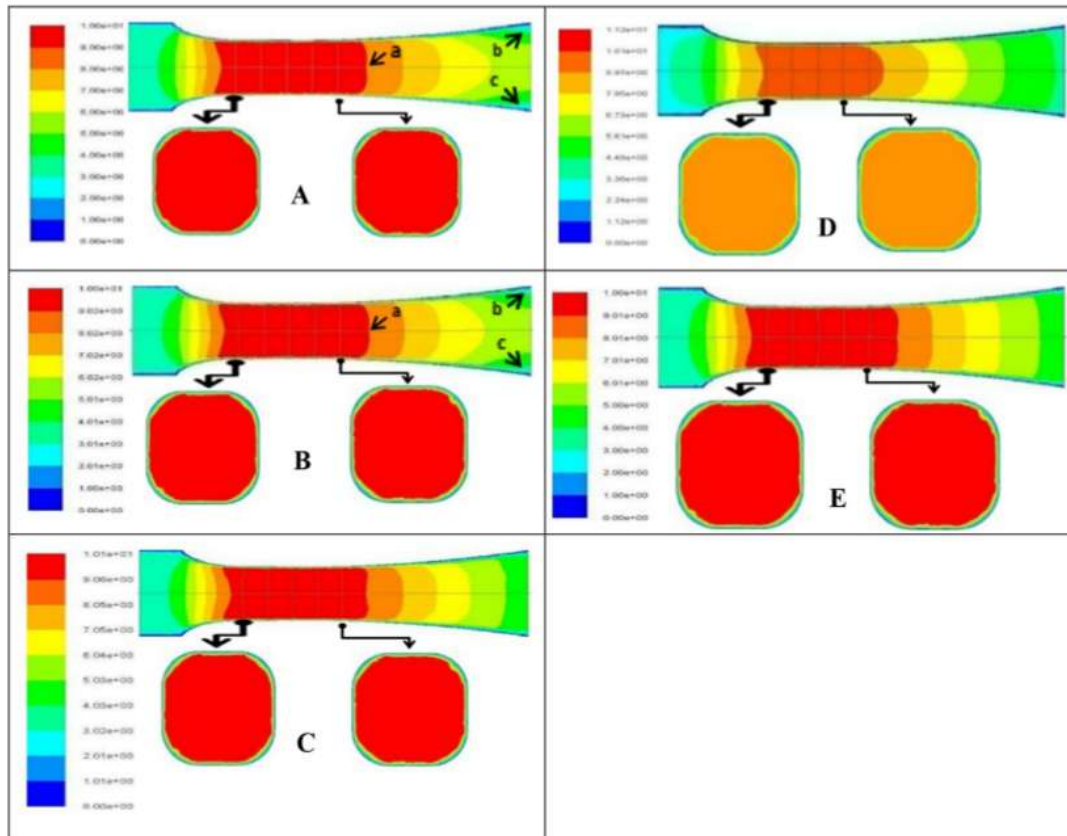

Fig. 4. The sequential velocity distribution of each model k-ϵ (a), k-ω (b), RSM (c), SST k-ω (d), LES (e) at U_0 = 3.3 m/s.

value computed from mathematical calculations (Bernoulli continuity law). Then, the results are used as input in the simulation to obtain a velocity distribution model in the wind tunnel, especially the variation of airflow in the test chamber. In this study, 2 desired airflow data in the test room are 10 m/s, and 20 m/s.

The wind tunnel geometry in this study has the length L is 5.628 m, the cross section length is 1.245 m square and the edges are curved with radius 0.250 m, so the wind tunnel volume is 4.60×10^6 m³ and surface area is 2.13×10^5 m² (Fig. 1). The cross section of the output gap of the diffusion chamber is determined to equal the area of the cross section of the gap entering the contraction chamber. Whereas the fan is located after the diffusion chamber has a diameter of 1.250 m, has a maximum flow rate of 8.75 m³/s.

5. Results and discussion

Some research has been carried out to design and investigate wind tunnels, but they are more focused only on the scheming contraction parts [4,26–28]. There are also reviews of the wind tunnel that only want to provide a general description of the distribution of airflow in the wind tunnel [29] to prove the laminar flow protection and there is no review on how to determine the position of the test object in the test chamber. The four sides of the wind tunnel in

this analysis are curved on their side (⌀ 50 cm), distinguishing them from the geometry of the wind tunnel in another review where the tested wind tunnel has angles on all four sides.

The velocity contour patterns achieved in the test section vary for each turbulence model as shown in Fig. 4. The initial velocity of 3.3 m/s Fig. 4 is also different in velocity distribution contours for the initial velocity given at 6.6 m/s (Fig. 5). The pattern of velocity distribution in the test section shows different contours, both in terms of velocity and the turbulence model used. Model k-ε (Fig. 4. A) with arrow a shows the direction of the curvature trending into the test chamber due to axial flow and the tilt of the wall of the 5° diffusion chamber. This phenomenon is increasingly clear with increasing velocity in the test section (Fig. 5), the five models tend to occur backflow when entering the diffusion chamber. Symptoms of the boundary-field layer occur but do not appear to cause the separation flow, because the boundary-plane layer is pushed away until it approaches the end of the diffusion chamber (arrows b and c).

With an initial velocity of 3.3 m/s, a velocity corresponding to the estimate required in the tunnel test chamber is 10 m/s. Because the velocity of the fluid in the test chamber is expected to be in the range of 10 m/s − 20 m/s. The overall model consistently displays the velocity in the test section 10 m/s when the initial velocity is 3.3 m/s. Even the area covered by the red gradation exceeds the
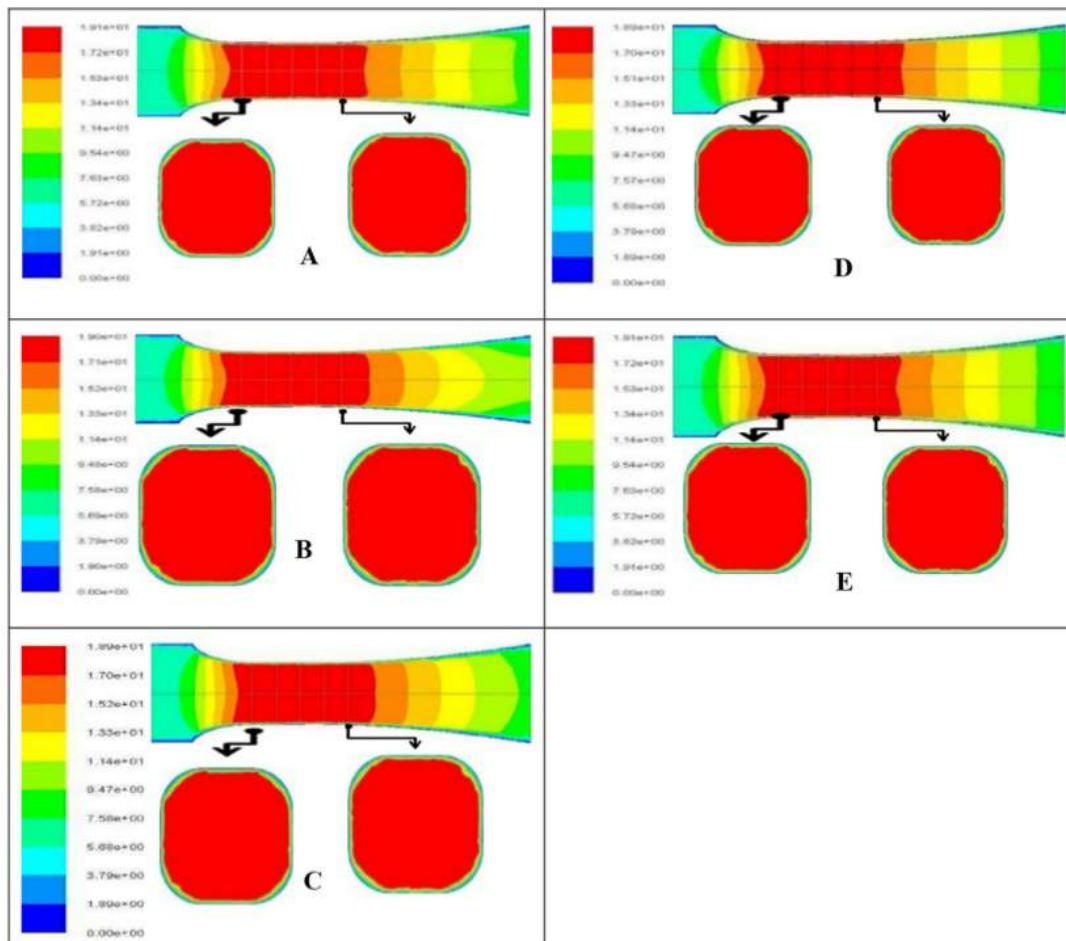

Fig. 5. The sequential speed distribution of each model k-ε (a), k-ω (b), RSM (c), SST k-ω (d), LES (e) for U_0 = 6.6 m/s.

E section ie the output of the test chamber and the input for the diffusion chamber. Arrows b and c display a layer of boundary fields pushed away from the test chamber and not as large as shown in Fig. 5. SST 33 model (Fig. 4.D) is shown in reddish-orange gradations for velocity of 10 m/s. The average velocity in the test section is given by the k-ϵ and k-ω models which are 9.98 m/s and 10.02 m/s compared to the other three models. The average velocity in the test chamber is 10.0 m/s, even the area covered by the red gradation exceeds the E section ie the output of the test chamber and the input for the diffusion chamber. There are similarities in the character of the SST k-ω model with the model k-ω model which is the tendency to round out the flow pattern when leaving the test section and enter the diffusion section. This similarity can be understood as the definition of both models, namely turbulent kinetic energy *k* and specific rate of dissipation ω.

The phenomenon of the boundary-field layer in the test section does not affect the pattern of fluid movement in the test chamber. This condition is caused by the large freestream velocity or the high Reynolds number in the test chamber suppresses the potential for increasing the thickness of the layer. Likewise, the suspicion of the influence of the asymmetry of space using unstructured mesh does not occur like ripples in a wind tunnel. The boundary-plane layer in Fig. 5 is pushed away to the diffuser area but does not affect the uniformity of fluid flow in the test chamber. When the fluid moves rapidly in the test chamber and when it passes through the cross-section E as the transition area, the flow velocity decreases with the hydraulic diameter D_h of the diffusion chamber increasing and is characterized by a slope of 5° towards the plane of the test chamber. Slowing velocity and the slope effect of the diffusion chamber produce trending backflow against the main-

stream. Thus a current is created due to the curvature effect or the curvature effect of the fluid pass field. All models of turbulence and the results of mathematical calculations show the velocity of the fluid more or less the same in the contraction section, but then the tendency changes when it has passed through the contraction section.

The simulation results of the distribution of airflow in the contraction area in this study show air compatibility with the review conducted by Abdelhamed [4] using the SST k-ω model. The ratio of the air velocity to the distance amplified in the test chamber indicated by the previous report can also be compared with the results of this research. Removing the sharp angle geometry on all four sides of the wind tunnel to avoid the possibility of eddy flow, which is the simulation results from the cross-section (Figs. 4 and 5) do not show differences in the shape of distribution with Rodríguez Lastra [28].

The thickening appearance in Fig. 5 as a mechanism for increasing the boundary-field layer thickness and the sensitivity of the k-ω model (Fig. 5.B) towards freestream seems to indicate that the freestream flow pushes the fluid to form a boundary layer becomes longer and thickens at the end diffusion. Model k-ω has the advantage of modeling boundary-field layers caused by adverse pressure gradients and by eliminating the damping function, the model is stronger in constructing the flow around the wall [30].

Another parameter in determining the position of the test sample in the test room is the presence of visual data on the pressure distribution. Visual data distribution of the fifth static pressure turbulence model in wind tunnels at initial velocity of 3.3 m/s and 6.6 m/s (Fig. 7). The color stick shows the blue gradation is the lowest pressure in the tunnel, and the red gradation is the highest pressure. The five models of the two velocity show that the pressure decreases when entering the test section then increases when leaving the test section, although the pressure on each model varies.

At the average velocity of the test chamber 10 m/s, the magnitude of the pressure is the k-ϵ model giving the pressure value in the test section is −61.6 Pa, the k-ω model is − 64.4 Pa, the RSM model is −56.8 Pa, SST k-ω is − 31.2 Pa and the LES model is −62.8 Pa. Whereas for the average velocity of 20 m/s the model in the test section obtained for the k-ϵ model is

− 217.89 Pa, the model k-ω is − 231.22 Pa, the RSM model is − 231.22 Pa, the SST k-ω model is − 230.2 Pa and the LES model is 221.0 Pa.

The description of pressure dispersions in wind tunnels has a pattern that is consistent with Ahmed D.E., et al. essay [31], although Ahmed D.E. only takes the profile of half the wind tunnel. The results of the static pressure values differ but the pressure contour characteristics have a close visualization. The dominance of the blue gradations in the test section can be seen starting from cross-section B to cross-section E. The cross-section A has a pressure above the cross-sectional pressure values B, C, D, and E, except for the k-total model whose overall cross-section is dominated by blue (lowest pressure). So that to position objects in the test section is right when placed in the area between cross-section B and cross-section E, taking into account the uniformity of velocity and pressure that occurs in the wind tunnel test chamber. The cross-sectional area A has a maximum pressure distribution but in that area, there are still fluctuations in pressure or not entirely homogeneous so that positioning the specimen in the cross-sectional area will not be optimal because non-uniform pressure in the test chamber is one of the disturbances. Then determining the position of the sample in the area between cross-section B and cross-section E is correct and optimal.

The negative gradient by the graph of the turbulence intensity of the five turbulence models is shown in Fig. 8. If the velocity curve in Fig. 6 is the maximum curve and tends to be uniform, then
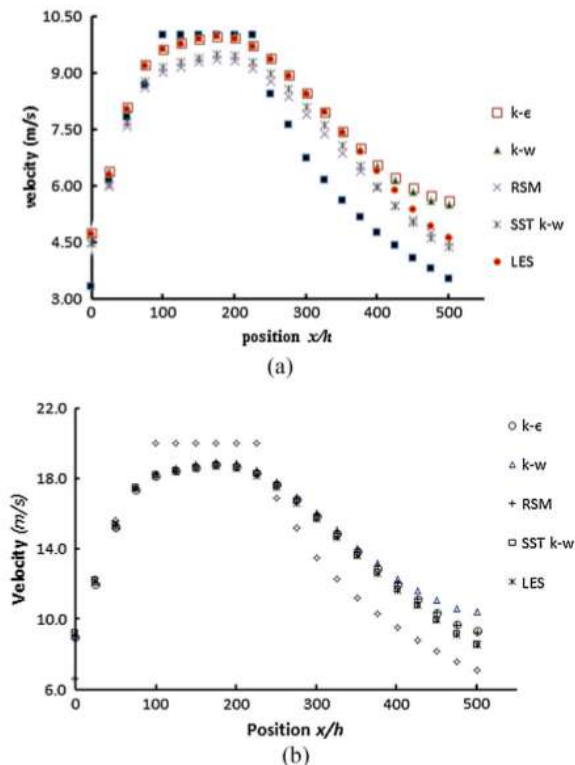

Fig. 6. Graphic U_0 = 3.3 m/s (a) and U_0 = 6.6 m/s (b) of fifth turbulence models.
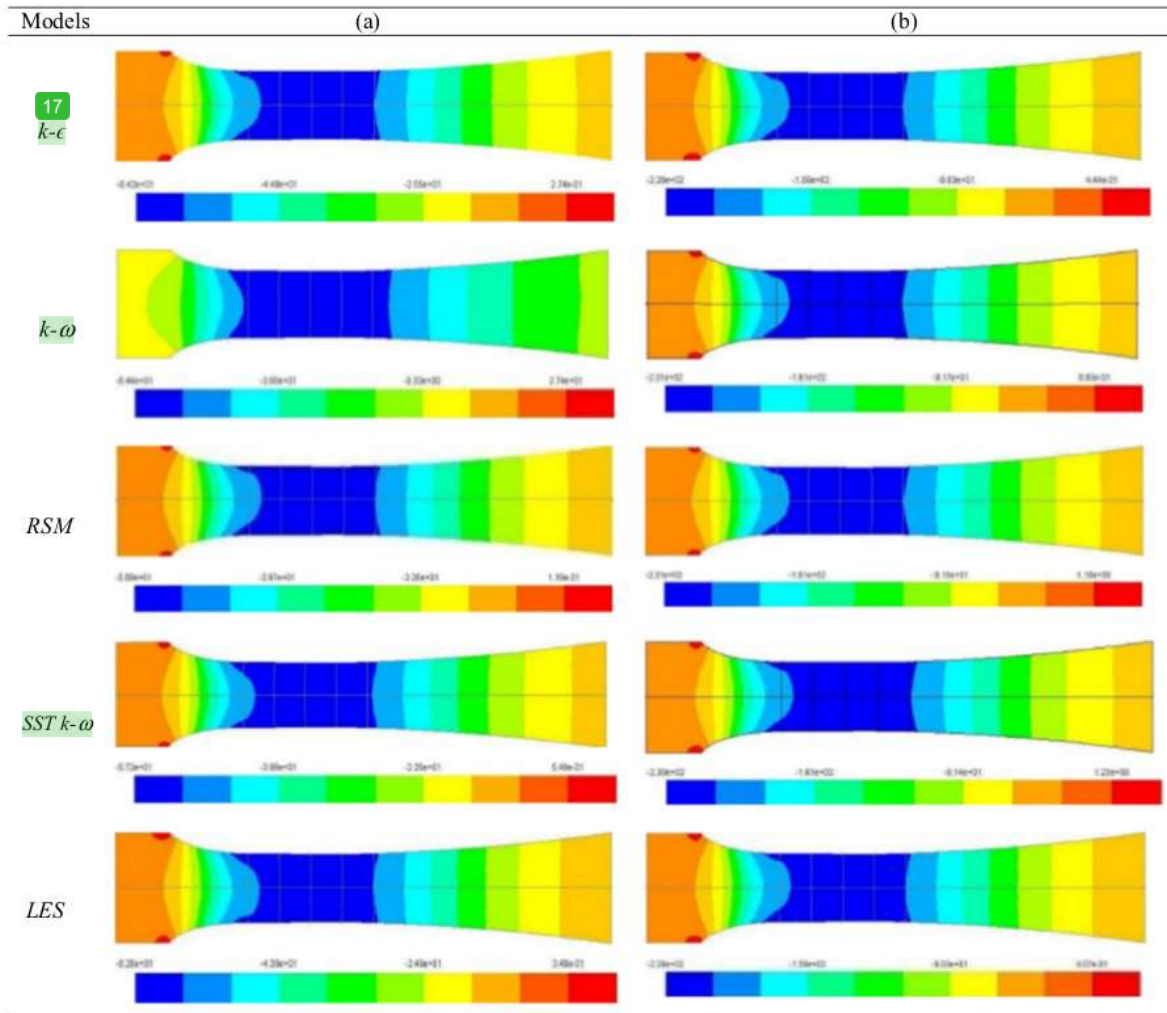
Models	(a)	(b)

Fig. 7. Pressure distribution at U_0 = 3.0 m/s (a) dan U_0 = 6.6 m/s (b).

the turbulence intensity curve of the five CFD method models varies. The LES model curve has the largest gradient with a sharp slope, except the other four turbulence models, form a gentle curve (small curve gradient). The high-intensity gradient of turbulence in the LES model has an impact on the level of turbulence produced in the test chamber, which is 16.3%. While the turbulence model which shows a small intensity value is given by the model k-ε with the intensity of turbulence in the test chamber is 0.8%. The turbulence rate of other models, namely the k-ω model is 13.5%, the RSM model is 3.5% and the SST k-ω model is 14.6%.

The turbulence intensity graph in Fig. 8, both at velocity of 10 m/s or 20 m/s, shows mixed results between each model. The LES model gives the value of turbulence intensity in the test section between 5.1% − 10.9%, the RSM model whose curves tend to be flat gives turbulence values between 2.3% − 2.9% in the test chamber and is the model with the smallest turbulence intensity compared to other models. The intensity value of turbulence by other models in the test chamber is 6.9% − 8.1% by the k-ω model, 2.6% − 3.2% by the k-ε model, and the SST k-ω 11.40%. The RSM model has an intensity value that is quite close the k-ε model and the turbulence intensity curve gradient of this model is also as small as the

k-ε model because of a more flat curve. The turbulence intensity curve of the SST k-ω model has the flattest tendency compared to the two previous curve models, the RSM model and the k-ε model. But overall, the direction of the turbulence intensity curve of the five turbulence models is negative. The k-ε model with the smallest turbulence intensity has a velocity range in the test chamber is 18.14 m/s − 18.79 m/s while the LES model which has a high turbulence gradient, the velocity range is shown in the test chamber is 18.15 m/s − 18.67 m/s.

6. Conclusion

Evaluation of the use of CFD simulations in wind tunnel designs gives reliable results, especially if the results are compared to previous studies. Each investigation uses a different model but the results obtained are not much different, especially in the utilization of parameters and methods that have similarity characteristics. This condition is important for some turbulence models in order to get a comprehensive concept of air flow.
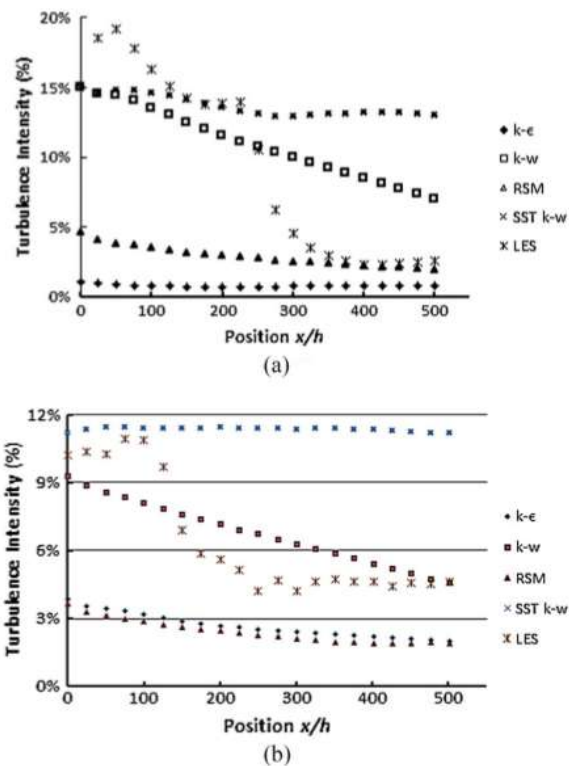
Fig. 8. Turbulence Intensity Chart of five turbulence models on U = 10 m/s (a) dan U = 20 m/s (b).

The turbulence level of the five models of the 2 output velocity in the test room, for velocity of 10 m/s in the test space such the k-ε model is 3%, the k-ω model is 14%, the RSM model is 4%, SST k-ω is 15% and the LES model is 18%. For velocity of 20 m/s, the k-ε model is 3.2%, the k-ω model is 8.1%, the RSM model is 2.9%, the SST k-ω is 11.4% and the LES model is 10.9%. Then the intensity of turbulence in wind tunnel test sections is still high because some models provide values above 10%, although there are symptoms of decreasing the value of turbulence intensity as the flow velocity increases in the wind tunnel. The ideal turbulence intensity has not been obtained from this simulation which is below 1%, so analysis of wind tunnel design is needed again, especially in the contraction space. Some adjustments are needed to the geometry and design of the contraction chamber structure, but it is also possible in other spaces such as diffusion spaces.

The velocity distribution in the test section is more evenly distributed, as for the initial velocity of 3.3 m/s, the velocity in the k-model model test section shows the maximum velocity achieved is 9.98 m/s, the k-ω model is 9.98 m/s, RSM model at 10.0 m/s, the SST k-ω model is 11.2 m/s and the LES model is 10.2 m/s. At the initial velocity of 6.6 m/s the maximum velocity obtained from the simulation result is that the model k-ε is 19.1 m/s, the model k-ω is 19.0 m/s, the RSM model is 18.9 m/s, SST k-ω is 18.9 m/s and LES are 19.1 m/s.

The simulation results in the form of velocity distribution contours and pressure distribution within the wind tunnel test room show that the optimal position of the test specimen is between the B and D cross-sections. The RSM model that is superior in modeling the interaction between strain and stress components in fluid flow does not show presence boundary-plane layer and followed by the SST k-ω model and the LES model. The RSM model, similar to the k-ε model, shows a low level of turbulence in the test chamber. Whereas the other models, namely the LES model, the SST k-ω model, and the k-ω model provide the value of the turbulence level above the two models.

Declaration of Competing Interest

The authors declare that there are no conflicts of interest regarding the publication of this paper

Acknowledgement

References

[1] Ismail Kamal S, Purnomo Sarjiya, Tampubolon S, Azmi AA, et al. Modification of open circuit wind tunnel. ARPN J Eng Appl Sci 2015;10:8150–6.

[2] Ismail John J, Libyawati W, Rhakasywi D, Suwandi A, Hendrayanto P. Optimization Design of Open Circuit Wind Tunnel Suction Type. Int J Mech Mechatr Eng 2017;17:121–31.

[3] Rhakasywi D, Ismail Suwandi A, Fadhli A. Analysis of subsonic wind tunnel with variation shape rectangular and octagonal on test section. IOP ConfSer: Mater Sci Eng 2018;308:1–10. doi: https://doi.org/10.1088/1757-899X/308/1/012036.

[4] Abdelhamed AS, Yassen YE, Elsakka MM. Design optimization of three dimensional geometry of wind tunnel contraction. Ain Shams Eng J 2015;6:281–8. doi: https://doi.org/10.1016/j.asej.2014.09.008.

[5] Chen X, Hussain F, She Z. Predictions of canonical wall-bounded turbulent flows via a modified k – ω equation ARTICLE HISTORY. J Turbul 2017;18:1–35. doi: https://doi.org/10.1080/14685248.2016.1243244.

[6] Aupoix B. Roughness Corrections for the k – w Shear Stress Transport Model : Status and Proposals. J Fluid Eng 2015;137:1–10. doi: https://doi.org/10.1115/1.4028122.

[7] Farouk MI. Check the comfort of occupants in high rise building using CFD. Ain Shams Eng J 2016;7:953–8. doi: https://doi.org/10.1016/j.asej.2015.06.011.

[8] Ahsan M. Computational fluid dynamics (CFD) prediction of mass fraction profiles of gas oil and gasoline in fluid catalytic cracking (FCC) riser. Ain Shams Eng J 2012;3:403–9. doi: https://doi.org/10.1016/j.asej.2012.04.003.

[9] Blocken B, Stathopoulos T, Van Beeck JPAJ. Pedestrian-level wind conditions around buildings : Review of wind-tunnel and CFD techniques and their accuracy for wind comfort assessment. Build Environ 2016;100:50–81. doi: https://doi.org/10.1016/j.buildenv.2016.02.004.

[10] Menter FR. Two-Equation Eddy-Viscosity Turbulence Models for Engineering Applications. AIAA J 1994;32:1598–605. doi: https://doi.org/10.2514/3.12149.

[11] Jawarneh AM, Vatistas GH. Reynolds Stress Model in the Prediction of Confined Turbulent. J Fluid Eng 2006;128:1377–82. doi: https://doi.org/10.1115/1.2354530.

[12] Vemula JB, Sinha K. Reynolds stress models applied to canonical shock-turbulence interaction. J Turbul 2017;18:653–87. doi: https://doi.org/10.1080/14685248.2017.1317923.

[13] Olsen ME, Lillard RP. Murman SM. Prediction of Large Separations with Reynolds Stress Models. Fluid Dynamics and Co-located Conferences, San Diego: American Institute of Aeronautics & Astronautics 2013:1–22.

[14] Hallback M, Sjogren T, Johansson AV. Turbulent Shear Flows 9. Kyoto: Springer; 1993.

[15] Knochenhauer TJ, Kornev SKRN. Coupling of Human Thermoregulation and URANS Computation for Investigation of Local Heat Transfer and Flow Structures in a Generic Car Cabin Flow. Turbul Combust 2016;97:1281–96. doi: https://doi.org/10.1007/s10494-016-9780-z.

[16] Palkin E, Mullyadzhanov R, Hadziabdic M, Hanjalic K. Scrutinizing URANS in Shedding Flows : The Case of Cylinder in Cross-Flow in the Subcritical Regime. Flow Turbul Combust 2016. doi: https://doi.org/10.1007/s10494-016-9772-z.

[17] Yik K, Stewart L. Assessment of LES Subgrid-scale Models and Investigation of Hydrodynamic Behaviour for an Axisymmetrical Bluff Body Flow. Flow. Turbul Combust 2016. doi: https://doi.org/10.1007/s10494-016-9751-4.

[18] Bradshaw P. Turbulence Modeling with Application to Turbomachinery. Prog Aerosp Sci 1996;32:575–624.

[19] Argyropoulos CD, Markatos NC. Recent advances on the numerical modelling of turbulent flows. Appl Math Model 2015;39:693–732. doi: https://doi.org/10.1016/j.apm.2014.07.001.

[20] Anonim. ANSYS: Tutorial Guide. 2012.

[21] Wilcox DC. Formulation of the k -w Turbulence Model Revisited. AIAA J 2008;46:2823–38. doi: https://doi.org/10.2514/1.36541.

[22] Davidson L. An Introduction to Turbulence Models. 1st ed. Goteborg: CHALMERS; 2018.

[23] Hanjalic K, Launder BE. A Reynolds stress model of turbulence and its application to thin shear flows. J Fluid Mechanical 1972;52:609–38.

[24] Lim DC, Al-kayiem HH. Kurnia JC. Comparison of different turbulence models in pipe flow of various Reynolds numbers. In: AIP Conference Proceedings 2035. AIP Publishing; 2018. p. 1–9. 10.1063/1.5075553.

[25] Hussain S, Oosthuizen PH, Kalendar A. Evaluation of various turbulence models for the prediction of the airflow and temperature distributions in atria. Energy Build 2012;48:18–28. doi: https://doi.org/10.1016/j.enbuild.2012.01.004.

[26] Bradshaw P, Pankhurst RC. The Design of Low Speed Wind Tunnels. Teddington 2012.

[27] Vladimíra M, Sergej KĚT, Ji B. Numerical and Experimental Investigations of Air Flow Turbulence Characteristics in the Wind Tunnel Contraction. Appl Mech Mater 2014;617:275–9. doi: https://doi.org/10.4028/www.scientific.net/AMM.617.275.

[28] Rodríguez M, Manuel J, Oro F, Vega MG, Marigorta EB, Morros CS. Novel design and experimental validation of a contraction nozzle for aerodynamic measurements in a subsonic wind tunnel. Jnl of Wind Engineering and Industrial Aerodynamics 2013;118:35–43.

[29] Hernández MAG, López AIM, Jarzabek AA, Perales JMP, Wu Y, Xiaoxiao S. Design Methodology for a Quick and Low-Cost Wind Tunnel. INTECH 2013:3–28.

[30] Menter FR. Influence of Freestream Values on k-w Turbulence Model Predictions. AIAA J 1991;30:1657–9.

[31] Ahmed DE, Eljack EM. Optimization of Model Wind-Tunnel Contraction Using CFD. 10th International Conference on Heat Transfer, Fluid Mechanics and Thermodynamics, Orlando: HEFAT. p. 87–92.

Computational fluid dynamics simulation of the turbulence models in the tested section on wind tunnel

8 dsp.tecnalia.com
Internet Source
1%

9 idoc.pub
Internet Source
1%

10 www.mdpi.com
Internet Source
<1%

11 Akansu, S.O.. "Heat transfers and pressure drops for porous-ring turbulators in a circular pipe", Applied Energy, 200603
Publication
<1%

12 van Hooff, T., B. Blocken, and G. J. F. van Heijst. "On the suitability of steady RANS CFD for forced mixing ventilation at transitional slot Reynolds numbers", Indoor Air, 2013.
Publication
<1%

13 publications.lib.chalmers.se
Internet Source
<1%

14 L. Chang-geng. "Experimental and Numerical Simulation Study of Heat Transfer Due to Confined Impinging Circular Jet", Chemical Engineering & Technology, 10/2007
Publication
<1%

15 Submitted to De La Salle University - Manila
Student Paper
<1%

16 César Porras-Amores, Carmen Viñas-Arrebola,

Antonio Rodríguez-Sánchez, Paola Villoria-Sáez. "Assessing the potential use of strategies independent from the architectural design to achieve efficient ventilation: A Spanish case study", Building Services Engineering Research and Technology, 2014
Publication

17 Yigang Sun, Zhongchao Tan, Yuanhui Zhang, Lingying Zhao. "Comparison of Six CFD Models for Room Airflow Study with PIV measurement Data", 2004, Ottawa, Canada August 1 - 4, 2004, 2004
Publication

18 "Recent Advances in Theoretical, Applied, Computational and Experimental Mechanics", Springer Science and Business Media LLC, 2020
Publication

19 Tackling Turbulent Flows in Engineering, 2011.
Publication

20 Submitted to City University
Student Paper

21 Sundaram, S. Soma, and V. Babu. "Numerical Investigation of Combustion Instability in a V-Gutter Stabilized Combustor", Journal of Engineering for Gas Turbines and Power, 2013.
Publication

22 jurnal.umsu.ac.id
Internet Source
<1%

23 Xiuli Mao, Ze Liu, Ting Li, Gaojun Mao, Diyi Chen. "A brief review of numerical solving methods for internal fluid of pumped storage unit", International Journal of Energy Research, 2020
Publication
<1%

24 Mahmood Silieti, Eduardo Divo, Alain J. Kassab. "The Effect of Conjugate Heat Transfer on Film Cooling Effectiveness", Numerical Heat Transfer, Part B: Fundamentals, 2010
Publication
<1%

25 B. Blocken, T. Stathopoulos, J.P.A.J. van Beeck. "Pedestrian-level wind conditions around buildings: Review of wind-tunnel and CFD techniques and their accuracy for wind comfort assessment", Building and Environment, 2016
Publication
<1%

26 Sanjeev K. Jha, Fabián A. Bombardelli. "Two-phase modeling of turbulence in dilute sediment-laden, open-channel flows", Environmental Fluid Mechanics, 2009
Publication
<1%

27 Huang, Yi, Qibin He, Huiyuan Shen, and Yanhua Liu. "Effect of the Fence of Urban Residence Communities on the Diffusion of
<1%

Ground Pollutants", Lecture Notes in Electrical Engineering, 2014.
Publication

28 mafiadoc.com
Internet Source
<1%

29 Xiao, Qi, Ning Yang, Jiahua Zhu, and Liejin Guo. "Modeling of cavern formation in yield stress fluids in stirred tanks", AIChE Journal, 2014.
Publication
<1%

30 Wang, Bingxu, Weihong Zhang, Gongnan Xie, Yingjie Xu, and Manyu Xiao. "Multi-configuration Shape Optimization of Internal Cooling Systems of a Turbine Guide Vane based on Thermomechanical and Conjugate Heat Transfer Analysis", Journal of Heat Transfer, 2014.
Publication
<1%

31 uknowledge.uky.edu
Internet Source
<1%

32 arc.aiaa.org
Internet Source
<1%

33 link.springer.com
Internet Source
<1%

34 Farzad Bazdidi-Tehrani, Mahdi Karami, Mehdi Jahromi. "Unsteady flow and heat transfer

analysis of an impinging synthetic jet", Heat and Mass Transfer, 2011
Publication

35 hdl.handle.net
    Internet Source   <1%

36 Jyeshtharaj B. Joshi. "CFD simulation of stirred
    tanks: Comparison of turbulence models. Part I: <1%
    Radial flow impellers", The Canadian Journal of
    Chemical Engineering, 02/2011
    Publication

37 Emmanuel Guilmineau, Patrick Queutey.
    "Numerical Study of Dynamic Stall on Several   <1%
    Airfoil Sections", AIAA Journal, 1999
    Publication

Exclude quotes   Off   Exclude matches   Off
Exclude bibliography   On